Deep Learning-Driven Virtual Clothing Fit Detection and Automatic Pattern Correction Technology

Yueli Li[1], Nan Wu[2], Zhuangyan Qiu[1]
[1]College of Textiles & Clothing, Yancheng Polytechnic College, Yancheng 224005, Jiangsu, China
[2]Information Technology Center, Yancheng Polytechnic College, Yancheng 224005, Jiangsu, China
Corresponding author: Yueli Li (e-mail: lyueli2021@163.com)

ABSTRACT Online fashion platforms continue to experience significant refund rates due to inaccurate virtual fit assessments and the lack of integrated, automatic Fabric Pattern Adjustment. Existing virtual try-on methods typically rely on 2D image alignment and mesh-based simulations, which provide poor collision awareness and inefficient large-scale deformation modelling. To solve the above issue, this Work introduces a unified Deep Learning Framework (SDF-FNO) that combines a Signed Distance Function (SDF)-based neural network for virtual clothing fit identification and a Fourier Neural Operator (FNO) for automatic garment pattern correction. The SDF network uses collision-aware surface evaluation to determine tight, normal, and loose fit zones by modelling the human body and garment as continuous implicit surfaces and computing signed distance differences. The FNO learns to modify the entire garment pattern at once, then reconstructs a smooth, corrected pattern by analysing global shape changes in the frequency domain. The system is trained and tested using the 4D-DRESS dataset, which contains dynamic 3D clothed human scans. The SDF-FNO demonstrates scalability across e-commerce virtual try-on, augmented-reality retail, digital tailoring, and intelligent clothing production systems. The experimental results show 94.6% fit classification accuracy, 93.9% automated pattern correction success rate, and 94.3% overall application-level accuracy, while maintaining stable real-time inference performance.

INDEX TERMS signed distance function (SDF), fourier neural operator (FNO), virtual try-on systems, automatic garment pattern correction, 3D cloth simulation

I. INTRODUCTION

THE textile and garment sector is increasingly adopting digital platforms because clothing fit and pattern accuracy affect consumer satisfaction, brand credibility, and market competitiveness [1]. More people purchase online and use size guides and product photographs, making dressing less critical. Understanding fabric behavior, choosing the proper size, and buying garments that fit is difficult [2]. However, ill-fitting clothes still account for a large share of product returns, which lowers productivity and increases costs for firms [3]. Recent research on AI-powered fashion tech and deep learning-powered virtual try-on systems suggests online shops require advanced fit prediction and visualisation frameworks [4]. AI-based pattern-sizing and fit solutions are essential for the textile industry to remain competitive and sustainable [5].

Size charts and hand pattern grading have been used for clothing fits. These approaches assume proportional size groups [6]. However, everyone differs in size, shape, and posture [7]. People are using smart clothing fit-detection technologies and digital simulations to reduce the need for physical samples and improve fit evaluations [8]. These technologies improve preview accuracy but still require designer and human correction, making automation and scalability difficult.

Due to processing resources, high-resolution virtual try-on systems aren't suitable for real-time online shop ping [9]. Fabric behavior depends on thickness, elasticity, and weave. A body data-driven garment pattern design study suggests adaptable, data-driven pattern-refining methods for various body types and apparel types.

Today, frameworks are judged by their appearance rather than their fit. It replicates how garments appear on virtual avatars without altering pattern geometry to achieve a better fit. This delays production-ready models and pattern revisions. Advanced deep learning-powered virtual try-on models improve garment realism [10]. Modeling and visualization have an improved framework that integrates automated pattern rectification and flawless match detection. Deep learning-based research on garment design re-editing emphasizes automated structural changes to ensure manufacturability and construction integrity. For scalable, end-to-end fit enhancement, textile marketing systems require a single foundation for automated pattern correction and precise fit identification.

This smart, scalable technology can identify ill-fitting garments and redesign them. This article examines bodyclothes imbalances and mismatches and makes improvements. More consistent digital garment previews and production outputs provide accurate sizing recommendations and targeted marketing. Experiments show that controlled-environment clothes are more authentic, consistent, and comfortable. By reducing fit issues before production, the SDF-FNO reduces return rates, optimizes resources, and builds customer confidence. The primary objective is i. To develop a scalable, real-time framework that is suitable for digital textile marketing and modern clothing manufacturing systems. ii. To create an SDF-based neural network that can effectively detect garment-body fit across several morphological categories. iii. To transform fit issues into economically viable and producible pattern modifications using a Fourier Neural Operator (FNO). iv. Generated patterns increase virtual try-on realism, improve fit accuracy, and reduce deformation errors, which lowers the possibility of returns and boosts customer satisfaction.

SDF-based neural networks identify garment fit, and Fourier Neural Operators (FNOs) correct patterns in the unified SDF-FNO framework. It uses dynamic 3D photos of clothed human bodies from the 4D-DRESS collection. The SDF-based network models garment-body interactions in continuous three-dimensional space using a signed distance field. Positive values indicate looseness, negative values penetration, and near-zero values acceptable contact. This enables the network to construct precise-fit deviation maps that show local and global deformation trends across body forms and clothing types. Automated pattern correction based on FNO refines garment patterns by analyzing fit discrepancies. With the help of a spatial pattern converter, the FNO can capture both large-scale deformation patterns and minute localized alterations. To restore patterns consistently and seamlessly, learnable spectrum filters modify frequency components. Computing expenses may be reduced without sacrificing accuracy or structural integrity by optimal spectrum processing. The paper is organized as follows. In Section II, the Literature Survey examines the literature on pattern correction, digital garment simulation, and garment fit analysis. Section III explains the overall system design, the dataset, the fit-detection technique, and automatic pattern refinement. Section IV shows the experimental results and comparative analysis. Section V includes a conclusion, suggestions for future research, and potential industrial applications; Section VI provides references for proceeding with this work.

II. LITERATURE SURVEY

V. B. Aakash et al (2024) [11] suggested Clothing Detection, Recommendation Systems, and Virtual Try-On Solutions based on AI-driven fashion technologies. The analysis covered deep learning-based garment detection models, a personalised recommendation system, and real-time virtual try-on models. The framework appears to improve customer interaction by providing real, simulated try-on experiences, customized recommendations, and a high detection rate. Performance shows a significant improvement in user customization and detection. Nonetheless, the survey points to the drawbacks of existing AI-based fashion systems in scalability, dataset diversity, computational efficiency, and the ability to perform structural modifications to clothing. T Islam et al. (2024) [12] developed deep learning-based virtual try-on models that are classified into imagebased, multi-pose, and video models; they examined architectures, data sets, evaluation metrics, and crossplatform performance comparisons. The researchers found improvements in client involvement, realism, and garment alignment. Nevertheless, it found deep-seated issues with texture retention, accuracy of body-garment warping, reliability of face identification, bias in datasets toward certain demographics, computational cost, and reduced generalization in real-world retail settings.

M. Servi et al. (2024) [13] investigated the application of artificial intelligence and augmented reality to improve conventional textile inspection. Evaluated automated defect-detecting algorithms, evaluated appro priate hardware design related to ergonomics and system efficiency, and designed a full AR-based inspection system. Their results showed that integrating AI and AR technologies enhanced defect-detection accuracy and reduced operators' workload in contemporary textile production facilities. Nonetheless, scalability in an industrial setting, fabric changes, and sensitivity to imaging conditions are limited.

S. Mei et al. (2018) [14] proposed a multi-scale convolutional denoising autoencoder for detecting and localizing fabric defects using an automated method. An unsupervised algorithm that relies on reconstruction residuals to detect defects on the pixel level and reconstruct image patches on different levels of resolution. The method was also able to handle numerous types of fabric, achieved increased stability through multiscale integration, required perfect samples for training, and delivered high accuracy with reliable recall in the experimental outcomes. The drawbacks are bad performance with highly textured materials and extensive training data requirements.

A work published by MDPI was by W.R. Wang et al. (2022) [15], who developed a real-time automated optical inspection system used to inspect woven fabric production lines. They employed a CMOS industrial camera and a four-step image processing pipeline that included the preprocessing, adaptive binarization, morphological features extraction, and SVM-based classification. This approach identified diverse types of woven fabric problems. It achieved high-quality detection with a low false-alarm rate, indicating that it can be used in practical textile production settings. Among the challenges are reliance on camera calibration, sensitivity to lighting changes, and difficulty detecting small defects. R. Carrilho et al (2024) [16] provide a diverse set of fabric photos and types of defects gathered at a Portuguese textile factory, as their contribution to closing the gaps in the recognition of anomalies based on a new fabric defect data set. To assess the feasibility of state-of-the-art deep learning methods for anomaly detection on complex, textured materials, they applied these methods to this dataset. The findings revealed large performance disparities and persistent challenges, underscoring the dataset's importance for comparing and extending research on fabric defect identification. Nonetheless, it requires further enhancement to accommodate extremely rare or complex defects.

K.H. Foysal et al. (2021) [17] developed an interactive mobile application to identify garment fit using image processing and machine learning, relying solely on smartphone images. The application assists in providing the best garment-fit recommendations and in solving sizing and returns issues when purchasing products online. Their initial analysis proved highly successful in identifying body shapes, enabling the system to address fit issues for online clothing companies. The challenges stem from the smartphone's camera, lighting, and limitations in capturing complex poses or multi-clothing situations.

An automated inspection system by J. Xiang, R. Pan, and W. Gao (2022) [18] consists of an enhanced deeplearning detection model and a dedicated image acquisition model for online detection of fabric flaws, based on an advanced CenterNet model with deformable convolution. They introduced a more effective feature pyramid network to handle multi-scale defects and a deformable convolution to handle various defect patterns. Experimental tests demonstrated that the proposed alternative achieved a reasonable trade-off between detection rates and processing time, indicating that it can be used to assess real-time industrial fabrics. Some of the limitations include dependence on camera calibration, sensitivity to lighting changes, and an inability to detect small errors.

H. Sun et al (2023), [19] proposed a digital simulation and re-editing approach to clothes patterns on deep learning and somatosensory interaction. The framework included diffusion-based image synthesis, an improved VGG19 architecture to support style migration, and 3D virtual dressing based on Kinetev2. They made clothes interactive to view, and patterns of coloured texture were reproduced. The experimental results revealed improvements in SSIM and PSNR, reduced colour overflow, accurate texture repair, and enhanced realism in virtual cloth modelling, and it mainly relies on pre-processed 3D models and necessitates decent computational specifications to handle complex clothing. Y. Gao (2023), [20] used a convolutional neural network to assess the beauty of clothing patterns and assist in design review by identifying and analyzing pattern types within a deep learning framework. To analyze performance differences, the method was compared with a standard back-propagation neural network. According to the experimental results, CNN worked better and faster. The proposed design scheme produced assessment outcomes that were quite comparable to human judgments, and test results demonstrated that it was highly accurate in identifying pattern styles. However, it requires unusual or unusual-looking designs and high-quality image datasets to achieve optimal performance.

Earlier research on garment fit detection and pattern correction did not generalize across body types, clothing shapes, and fabric properties, and made incorrect fit rulings. The issues caused high return and refund rates, increased production waste, inefficiency in online retail, large volumes of annotated data, a superabundance of computational resources, and human labor. These limitations underscore the need for more powerful, ver satile, and effective algorithms to identify fits and automatically correct patterns accurately. A Signed Distance Function (SDF)-based neural network and a Fourier Neural Operator (FNO) are combined to achieve accuracy, customization, and reliability in smart clothing garment-fitting methods and pattern-correction strategies. The SDF-based network is effective at detecting variability in fits across numerous morphological categories, using the 4D DRESS and 4D Human Datasets. The FNO model performs global spatial transformations and converts detected fit mismatches into structurally valid, manufacturable pattern repairs. The presented approach guarantees a high level of reliability, efficiency, and flexibility for digitally refining garments in apparel apps.

III. PROPOSED METHODOLOGY

The Signed Distance Function (SDF)-based network in this deep learning system analyzes virtual garment fit, and the Fourier Neural Operator (FNO) automatically corrects patterns. Rich vertex dynamics and semantic clothing labeling are available from 4D-DRESS and 4DHumanOutfit time-aligned models. Through a continuous implicit surface model, the SDF module discovers localized pressure areas, clearance margins, and penetration depth. A structured fit description is created by merging geometric discrepancy data across time. FNO then finds the spectral mapping between changes in garment pattern parameters and spatial discrepancies. The model learns smooth deformation and long-range interdependence. Pattern rectification that looks real and is appropriate for production requires accurate geometry and low error rates.

Figure 1 shows a hierarchical computational method for 4D garment fit analysis and automated pattern adjustment. The framework then accepts time-ordered motion sequences [21], garment meshes, and 3D human models [22]. These data records are combined to create a consistent 4D spatiotemporal representation [23] that captures the dynamic interactions between the body and garment, providing a basis for accurately predicting garment deformations under varying poses and movements. Preliminary processing stage (carries out geometric validation), the mesh is smoothed by removing noise and other geometrical errors, scale is normalized to induce uniformity across people, framewise strict spatial registration is performed by rotation and translation to align the body with the This, and time is enforced to make sure that modelling steps operate on representations

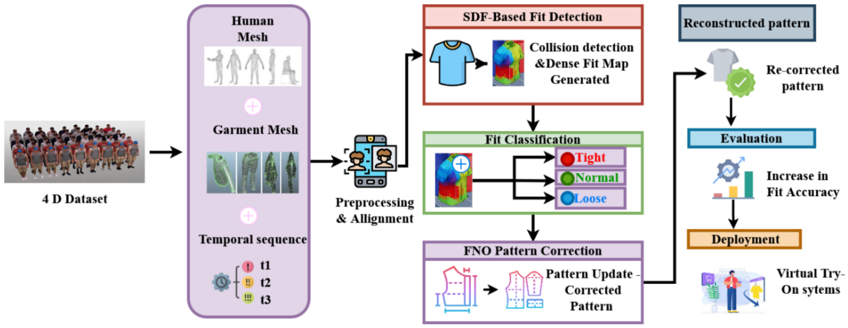

FIGURE 1. Overall Architecture of the SDF-FNO Framework

that are correctly positioned and structurally consistent. The data is preprocessed and aligned, and then processed by an implicit surface modelling module that utilises SDF [24]. This module calculates signed distance differentials to evaluate collision intensity and the distribution of clearance between the garment and the body [25]. The resulting map of the fit discrepancy provides a high-resolution, systematic understanding of the garment's deviation from a perfect fit. Then, the geometric discrepancy maps are fed into an (FNO)-based operator-learning module that learns global spatial transformations in the spectral domain. The FNO module provides smooth, concurrent, and consistent changes to the clothing design by translating local fit errors into world-scale, consistent deformation errors.

A. DATASET

The 4D dataset includes both temporal and spatial information, providing a 3D description of the human body and clothing over time. This sophisticated model allows us to investigate in depth the ways clothes deform, stretch, or even interact with the human body during different movements, postures, and activities. The 4D datasets are vital for analysing garment fit, replicating realistic clothing behaviour, and enabling applications such as virtual try-on and automated design alterations [26]. Let equation (1)-(2):

$$\text{Human mesh: } B(t) \in \mathbb{R}^{N_b \times 3} \quad (1)$$

$$\text{Garment mesh: } G(t) \in \mathbb{R}^{N_g \times 3} \quad (2)$$

where B(t) and G(t) are human and garment meshes, Nband Ngdenote the number of vertices in the body and garment meshes, respectively, and t= 1, 2, ..., Trepresents temporal frames. symbol Rrepresents the set of real numbers, 3 columns (x, y, z coordinates).

The dataset can be represented as equation (3):

$$D = \{(B(t), G(t)) \mid t = 1, 2, \ldots, T\} \quad (3)$$

Each frame records the topological structure, mesh connectivity, and accurate vertex location. To encode dynamic deformations such as stretching, compression, folding, and draping, the dataset analyzes a sequence of images. Temporal continuity enables accurate analysis of the evolution of garment patterns in relation to body motion, resulting in precise fit evaluation during realistic movements.

As seen in Figure 2, the 4D dataset helps explain garment evolution. The temporal 3D mesh sequences capture changes in human and apparel shapes across motion frames to ensure dynamic consistency. Using such patterns, vertex-level displacement fields may be calculated to calculate garment vertices' movements relative to the body, enabling precise research of stretching, compression, and directional deformation. Collision

and clearance maps illustrate skin-to-garment contact, penetration, and separation, assessing tightness and comfort. Dynamic deformation maps show folds, wrinkles, and draping patterns using color-coded surface alterations. The cloth reacts to movements. Drape, stretch ratio, contact area, and stiffness distribution are structural fit indicators. These findings provide the groundwork for automated digital pattern refinement and garment fit assessment in virtual try-ons.

B. PREPROCESSING & ALIGNMENT

The preprocessing and alignment stage converts raw 4D body-garment scan data into a geometrically consistent, accessible representation. As the dataset consists of time-varying 3D meshes, variations in noise, scale, spatial orientation, and temporal continuity can significantly affect subsequent SDF performance. To support SDF-based modelling, this module ensures temporal stability, normalization, and geometric regularization. The following steps are used to properly align the raw dataset, as shown in Figure 3.

1) Noise Removal

Noise removal is applied to eliminate scanning deviations, vertex disturbances, and high-frequency geometric variations found in the raw 4D clothing dataset. The dataset consists of a human body mesh and a garment mesh at each time step as B(t) $\in R^{Nb\times3}$, G(t) $\in R^{Ng\times3}$ and each row represents a 3D coordinate(x,y,z). A surface is generally represented in mesh form as follows equation (4):

$$M(t) = V(t), F \quad (4)$$

where V(t) = $\{v_i(t)\}_{i=1}^{N}$ represents the vertex coordinates a F represents face connectivity showing the mesh

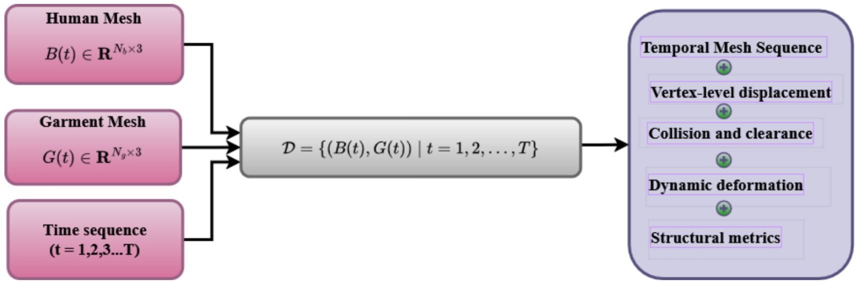

FIGURE 2. 4D Dataset Architecture

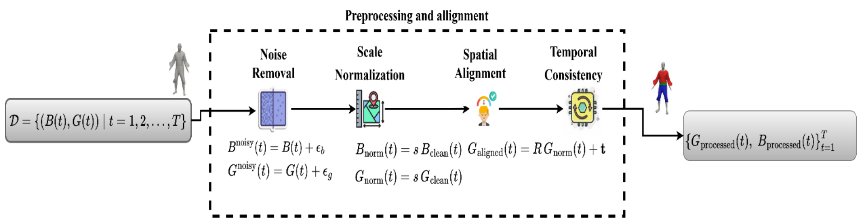

FIGURE 3. Preprocessing and Alignment block

topology. Each vertex is often corrupted by measurement noise, that is described as additive Gaussian noise in equations (5-6).

$$\theta_i^{noisy} = \theta_i + \epsilon_i \tag{5}$$

$$\epsilon_i \sim N(0, \sigma^2) \tag{6}$$

This formulation reveals that the observed vertex is equal to the genuine vertex plus a random disturbance with variation σ^2 has a zero mean, where the variance controls how much distortion arises. The noisy inputs in the dataset form can be written as follows equation (7):

$$B^{noisy}(t) = B(t) + \epsilon b, G^{noisy}(t) = G(t) + \epsilon g \tag{7}$$

Thus, the real input to the noise removal is $\{B^{noisy}(t), G^{noisy}(t)\}$ To minimize the high-frequency noise, Laplacian smoothing is used by maintaining geometric structure. The discrete Laplacian operator for every vertex is defined as equation (8):

$$\Delta\theta_i = \frac{1}{|N(i)|} \sum_{j \in N(i)} (\theta_j - \theta_i) \tag{8}$$

Where N(i) denotes the set of neighbouring vertices connected to vi, | N(i) | is the number of neighbours. This operator detects variations in the local curve by measuring a vertex's divergence from the average position of its local neighbourhood. Next, the vertex update rule is presented by equation (9):

$$\theta_i' = \theta_i + \lambda\Delta\theta_i \tag{9}$$

The smoothing coefficient $\lambda \in (0, 1)$ controls the strength of correction. This update moves each vertex a little closer to the centroid of its neighbouring vertices, thereby minimizing spikes and irregular oscillations while retaining the overall shape. The smoothing is applied separately for the dataset meshes as follows equation (10):

$$\begin{aligned} b_i' &= b_i + \lambda_b \Delta b_i, \\ g_i' &= g_i + \lambda_g \Delta g_i \end{aligned} \tag{10}$$

By applying the smoothing operation to all vertices, the cleaned meshes are obtained as in equation (11):

$$M_{clean}(t) = V_{clean}(t), F \tag{11}$$

The resultant meshes have no high-frequency noise, smoother geometry and they are numerically stable. This processed output provides precise data for the 4D framework's succeeding stages.

2) Scale Normalization

Body height, scanning setup, and reconstruction units still create scaled meshes after noise reduction. Global size discrepancies may bias signed Distance Function computations. By maintaining form proportions, scale normalization ensures that all meshes are the same size globally. Different vertical coordinates influence body height in equation (12):

$$H = max(y_i) - min(y_i) \tag{12}$$

where yi represents the vertical coordinate of body vertices. This equation measures the overall height of the body.

A scaling factor is defined with respect to a predefined reference height as H_{ref} fin equation (13):

$$s = \frac{H_{ref}}{H} \tag{13}$$

This ratio establishes the amount of uniform scaling required for the mesh.

The normalised mesh is represented as equation (14):

$$B_{norm}(t) = s \cdot B_{clean}(t), G_{clean}(t) = s \cdot G_{clean}(t) \tag{14}$$

The uniform scaling has the effect of multiplying all the coordinates by the same scalar, so that anatomical and clothing proportions are preserved. The resulting meshes are now all-dimensional across the dataset.

3) Spatial Alignment

The body mesh and the garment mesh may not align exactly after being normalized due to the differences in rotation or scanning position errors. Sound space alignment is needed to get accurate surface-to-surface distance calculations and collision analysis.

The alignment problem is expressed as a rigid transformation optimization problem.

$$\begin{aligned}(R^*, t^*) = \arg \min_{R\in SO(3),\, t\in\mathbb{R}^3} \sum_{i=1}^{N} \|b_i - (Rg_i + t)\|_2^2 \\ + \lambda \sum_{i=1}^{N} \|(Rg_i + t) - \bar{b}\|_2^2\end{aligned} \tag{15}$$

This equation (15) optimizes stiff body-garment vertex alignment. To get an appropriate rotation R*and trans lation t*for the goal function, square the distance between each body vertex b_i and the modified garment vertex $Rg_i + t$. For tight body mesh-garment mesh alignment, the vertex correspondence error is the first component. The second regularization term strives to align all garment vertices with the body mesh centroid $\bar{b}$ as closely as possible. Adjust the global limiting impact using the regularization parameter λ. This formula reduces the squared Euclidean distance between the modified garment vertices (g_i) and body vertces (b_i) . The rotation matrix adheres to the orthogonality constraint in equation (16):

$$\begin{aligned}\min_{R\in\mathbb{R}^{3\times3}} \left(\|R^T R - I\|_F^2 + \alpha(\det R - 1)^2 + \beta \sum_{i=1}^{3}\sum_{j=1}^{3} r_{ij}^2 \right), \\ \text{subject to } R \in SO(3)\end{aligned} \tag{16}$$

The rotation matrix used for body-clothing mesh spatial matching is accurate according to this equation. The first term $\|R^TR\text{-}I\|_F^2$ assures an orthogonal rotation matrix because R^TR-I maintains geometric distances and angles. The Frobenius norm causes the rotation matrix to preserve orthonormal column vectors to assess departure from the identity matrix. This requirement is met to avoid mesh distortion during scaling or shearing. By reducing the matrix determinant to one, the second term (det R-1)2 guarantees a rotation, not a reflection. The third regularization term stabilizes the optimization process $\sum_{j=1}^{3} r_{ij}^2$ that controls excessive parameter expansion in the rotation matrix. The optimization technique balances determinant and parameter regularization using weighting factors $\alpha$and β. Next, the aligned garment mesh is computed as:

$$G_{aligned}(t) = R^*(G_{norm}(t) - \bar{g}) + t^* + \bar{b} \tag{17}$$

The equation (17) estimates the optimum stiff transformation parameters received from the alignment optimization procedure and then computes the final aligned garment mesh. Rotation must revolve around the geometric center of the garment, hence the normalized garment mesh $G_{norm}(t)$ i s first centered by $\bar{g}$. After that, the ideal rotation matrix R* is used to realign the clothing mesh so subtracting its centroid that its spatial arrangement coincides with the body mesh's orientation. Using the ideal translation vector t*, the garment mesh is shifted to the right spatial location relative to the body surface after rotation. To move the garment mesh into the body model's global coordinate system, the centroid of the body mesh $\bar{b}$ is inserted last. This transformation makes sure that the body mesh and the clothing mesh are in the same spatial reference frame, that lets us calculate surface distances precisely, detect collisions, and analyze the interaction between the two. Through the use of centroid normalization in conjunction with stiff transformation, the process of alignment ensures the preservation of geometric structure while precisely situating the clothing mesh over the human body model. After this stage, the two meshes share a single coordinate system, that enables accurate geometric interaction analysis.

4) Temporal Consistency (4D Smoothing)

Since the dataset is dynamic, the location of the vertices changes dynamically. Nevertheless, small scanning errors can result in the temporal instability or other unforeseen changes between frames. Therefore, the temporal consistency is applied to give a smooth motion representation.

The following specifies a second-order temporal smoothness constraint:

$$\begin{aligned}L_{temp} = \sum_{i=1}^{N}\sum_{t=2}^{T-1} \frac{\theta_i(t+1) - 2\theta_i(t) + \theta_i(t-1)^2}{2} \\ + \gamma \sum_{i=1}^{N}\sum_{t=1}^{T-1} \|\theta_i(t+1) - \theta_i(t)\|_2^2\end{aligned} \tag{18}$$

This equation (18) temporal regularization loss function enables smooth mesh vertex movement between frames. First term exhibits second-order temporal difference, near-vertex discrete acceleration. Vertex shifts should be gradual between frames, this length must be lowered. The second component penalizes fast position changes between frames using first-order temporal consistency. To balance acceleration and velocity smoothing, a weighting value of γ is used. In this equation (18), the vertex i location at frame t is denoted as $\theta_i(t)$. The mesh has N vertices, T temporal frames, and γ regularization weight. This approach guarantees vertex trajectories remain consistent even when the body and garments move. The final processed dataset after noise removal, scale normalization, spatial alignment, and temporal smoothing is

$$D_{\text{processed}} = \{(G_{\text{processed}}(t), B_{\text{processed}}(t))\}_{\text{t=1,2,...,T}} \quad (19)$$

Noise reduction, scale normalization, spatial alignment, and temporal smoothing are formalized in this equation (19) for the processed 4D dataset. The dataset $D_{\text{processed}}$ contains the garment meshes $G_{\text{processed}}(t)$ and body meshes $B_{\text{processed}}(t)$ for each time frame t. The system organizes the dataset as time-ordered aligned mesh pairs to preserve body-clothing interaction geometry and continuity. This structured representation accurately models dynamic garment deformation throughout the whole motion sequence and offers dependable input for the Signed Distance Function calculation. This structured formulation offers reliable and consistent input for the 4D framework's intelligent garment fit analysis using Signed Distance Function computation.

C. SIGNED DISTANCE FUNCTION (SDF) - FIT DETECTION

Direct comparisons between these meshes may give unreliable and inconsistent results due to variations in the detail of the meshes, flaws in small surface areas, and time variation. In order to achieve a stable and precise evaluation, the body must be converted to an SDF representation. To achieve a geometrically accurate and constant evaluation. In this approach, rather than the simple surface shape, a smooth 3D field of numbers is obtained, where location searches can also be made powerful and reliable.

The signed distance at any spatial point p∈R3 is represented as equation (20):

$$D_B(p) = \min_{q \in \partial B(t)} \|p - q\| \cdot s(p) \quad (20)$$

where ∂B(t) represents the body surface, ‖p-q‖denotes the shortest Euclidean distance between point pand the body surface, and s(p) ∈{-1, +1} , the sign depends on whether the point lies outside or inside the body. This formulation assures that every point in space has a clearly defined distance value corresponding to the body surface.

Every vertex in the clothing is considered as a spatial query point in equation (21):

$$x_i = g_i(t) \quad (21)$$

where $g_i(t)$ represents the i[th] garment vertex.

Instead of comparing garment vertices to nearest body vertices, this step evaluates them directly within the continuous body distance field. This ensures geometric consistency even when the garment and body mesh have different resolutions.

The signed distance from the body is defined as equation (22):

$$d_i = D_B(x_i) \quad (22)$$

The high positive score indicates that the garment is loose and distant from the body. Zero values indicate an excellent fit. Negative values suggest body surface penetration. Continuous and surface-conscious exami nation yields more consistent findings than discrete collision testing.

The value d_i delivers a clear geometric explanation of garment fit. If $d_i > 0$, the garment vertex is outside the body surface, indicating a loose area. If $d_i = 0$, the vertex is directly on the body surface, indicating surface contact. If $d_i < 0$, the garment penetrates the body's surface, representing a collision. This signed interpretation offers the accurate localization of tight, loose, and penetration zones throughout the garment. By using this, a binary collision indicator can be indicated as equation (23):

$$C_i(t) = (d_i < 0) \quad (23)$$

This generates a vertex-by-vertex collision map all over the garment's surface. Negative signed distance indicates a penetration zone that needs to be corrected.

After the evaluation of each garment vertex, a dense distance map is generated.

$$D(t) = \{d_i\}_{i=1}^{N_g} \quad (24)$$

This equation (24) is produced on the cloth every time. When evaluated over temporal sequences, this creates a continuous 4D fit representation for collision detection, tightness estimation, and intelligent pattern correction. The SDF-based geometric model is resilient, persistent, and differentiable for exact garment fit analysis under dynamic situations. Algorithm 1 shows the SDF-Based Fit Detection.

Algorithm 1: SDF-Based Fit Detection

Input:
$\{G_{\text{processed}}(t)\}$ for $t = 1$ to T
1. For $t = 1$ to T do
2. $B \leftarrow B_{\text{processed}}(t)$
3. $G \leftarrow G_{\text{processed}}(t)$
Output:
$C \rightarrow$ Collision map
$D \rightarrow$ Signed distance map for garment vertices
\// Step 1: Construct Body Signed Distance Function
4. Construct SDF function $D_B(p)$ such that:
$D_B(p) = \min_{q \in \partial B(t)} \|p - q\| \cdot s(p)$
5. Initialize empty list $D(t)$, $C(t)$
\// Step 2 & 3: Garment Vertex Sampling and Distance Evaluation
6. For each garment vertex x_i in G do
7. min_distance $\leftarrow +\infty$

8. For each body surface point q in B do
9. distance $\leftarrow$ Euclidean Norm $(x_i - q)$
10. if distance $<$ min_distance then
11. min_distance $\leftarrow$ distance
12. end if
13. End for
\/ Determine sign
14. if x_i is inside the body surface then
15. sign $\leftarrow -1$
16. else
17. sign $\leftarrow +1$
18. end if
19. $d_i \leftarrow$ min_distance * sign
20. Append d_i to $D(t)$
\/ Step 4: Collision Detection
21. if $d_i < 0$ then
22. Append 1 to $C(t)$ // Collision
23. else
24. Append 0 to $C(t)$ // No collision
25. end if
26. End for
\/ Step 5: Dense Fit Map Generated
27. Store $D(t)$, $C(t)$
28. End for
29. Return $\{D(t)\}$, $\{C(t)\}$

The SDF pseudocode goes through each time frame (t=1,2,..., T) to look at the 4D garment-body sequence. The body mesh is initially converted to a Signed Distance Function $D_B(p)$ every frame. This converts the discrete surface representation into a 3D continuous scalar field. This stage ensures smooth, consistent, meshresolution-independent distance assessment. After that, each garment vertex $x_i \in G_{\text{processed}}(t)$ is treated like a point in space. The algorithm finds the shortest Euclidean distance between the garment vertex and the body surface. It then decides whether the vertex is inside or outside the body. The algorithm keeps track of these values for each frame and creates a binary collision map C(t) and a dense signed distance map D(t). Over again on all the frames get a 4D fit representation that is consistent over time. Then, the structured fit error field is sent to a Fourier Neural Operator (FNO), that makes global and smooth pattern corrections that slowly get rid of any fit inconsistencies that can be seen while keeping the garment's shape.

D. PATTERN CORRECTION USING FOURIER NEURAL OPERATORS (FNO)

Nevertheless, it is not enough to determine the inconsistencies in fit and apply these differences to the manufacturing of 2D pattern alterations. In order to achieve this, (FNO) is used to train a global map between the identified field of fit error and pattern corrections. The error field at the output of SDF is transformed into well-organized clothing pattern adjustments with the help of (FNO). To start with the dense signed distance map is transformed to a spatial error field, that represents tight and loose areas. This area is projected to the Fourier space that represents global spatial relations in terms of spectral representation. Learnable spectral weights modify the specified spectral modes to estimate an operator that projects fit errors to the deformation fields that have been fixed. A reverse Fourier transform is then used to convert the altered signal back to spatial space. Lastly, the garment pattern parameters are updated with the expected correction field, and the garment is enhanced for optimal fit. The spectral (Fourier) domain allows FNO to capture the global behaviour of deformations as well as long-range spatial dependencies, and is thus well-suited for refining clothing patterns.

The dense signed distance map attained from SDF detection in equation (25):

$$D(t) = \{d_i\}_{i=1}^{N_g} \tag{25}$$

The signed distance output from SDF is initially transformed into a structured fit error representation as equation (26):

$$E(t) = \phi(D(t)) \tag{26}$$

Where $\phi(\cdot)$ converts vertex-wise distances into a parameterized garment representation or spatial grid suit able for operator learning. The garment's tightness, looseness, and penetration intensity are encoded in this error area.

The error field is projected into the Fourier domain by equation (27):

$$\hat{E}(k) = \mathcal{F}(E(t)) \tag{27}$$

where $\mathcal{F}$ denotes the Fourier transform and k represents frequency modes.

This spectral form enables the model to incorporate global correlations, ensuring that pattern adjustments are made using the entire garment structure rather than isolated local regions.

The Fourier Neural Operator picks up a mapping in spectral space in equation (28):

$$\hat{U}(k,t) = \sum_{k' \in K} W(k,k')\hat{E}(k',t) + b(k) \tag{28}$$

The above equation (28) shows the Fourier Neural Operator's learnt spectral operator mapping. Translating the spatial fit error field $E(t)$ into the Fourier domain is important for producing a spectral representation $\hat{E}^{(k,t)}$. This field co mes from the SDF module. Instead of basic pointwise m ultiplication in frequency space, the operator uses the s pectral kernel $W(k,k')$ to map several frequency modes globally. This kernel's

modeling of frequency component interactions allows the network to recognize broad garment deformation patterns and more particular fit problems. In the spectrum domain, the updated correction field $\hat{U}^{(k,t)}$ indicates the expected deformation corrections. The bias term $b(k)$ stabilizes operator learning and improves training convergence. The Fourier Neural Operator learns frequency mode mappings like a continuous integral operator. This allows smooth pattern changes throughout the cloth. where $\hat{U}(t)$ is the transformed correction field, and $W(k)$ are spectral weights. This formulation approximates a continuous operator that transforms fit discrepancies into deformation adjustments over the entire garment domain.

After correction, the deformation field is converted back into spatial space in equation (29):

$$U(t) = \mathcal{F}^{-1}(\hat{U}(k)) \tag{29}$$

This results in a map of smooth spatial rectification across the clothing domain.

The final corrected pattern is defined as equation (30):

$$P_{\text{corrected}}(t) = P_{\text{initial}}(t) + U(t) \tag{30}$$

where U(t) is the expected adjustment field and (t) is the original pattern. This update adjusts panel widths, seam placements, and control positions to remove tight and loose sections identified by the SDF module. All FNO-based pattern repair modules integrate geometric fit flaws into global, automated pattern alterations. It enables continuous, smooth, resolution-independent modifications throughout dynamic 4D sequences since it acts in the spectral domain. Algorithm 2 describes the FNO Pattern Correction

Algorithm 2: FNO Pattern Correction

Input:
$D(t)$ — Dense signed distance map from SDF
$P_{\text{initial}}(t)$ – Initial garment pattern parameters
Model_Weights W — Learnable spectral weights
T — Number of time frames
Output:
$P_{\text{corrected}}(t) \rightarrow$ Updated garment patterns
1. For $t = 1$ to T do
2. // Step 1: Construct Fit Error Field
3. $E(t) \leftarrow$ Transform $(D(t))$.
\// Convert vertex-wise distances into a structured grid
4. //Step 2: Fourier Transform (Spectral Encoding)
5. $\hat{E}(t) \leftarrow$ Fourier Transform $(E(t))$
6. //Step 3: Spectral Operator Learning
7. For each selected frequency mode k do
8. $\hat{U}(k) \leftarrow W(k) * \hat{E}(k)$
9. End for
10. //Step 4: Inverse Fourier Transform
11. $U(t) \leftarrow$ Inverse Fourier Transform $(\hat{U})$
12. //Step 5: Pattern Update
13. $P_{\text{corrected}}(t) \leftarrow P_{\text{initial}}(t) + U(t)$
14. End for
15. Return $\{P_{\text{corrected}}(t)\}$

FNO_Pattern Correction uses SDF's dense signed distance map $D(t)$. Method turns geometric fit differences into structural advances in clothing design. For each time frame t, signed distance data is stored in a structured fit error field $E(t)$. This translation allows operators to compare vertex-wise distance data with a parameterized apparel domain to learn. The spatial error field is Fourier converted into the spectral domain. In this step, error distribution frequency components are separated. Low-frequency modes show global deformation patterns (overall looseness or tightness), while high-frequency modes show localized anomalies. During the spectral operator learning stage, trainable weights $W(k)$ change certain Fourier modes to create a continuous mapping between input fit errors and output corrective fields. The inverse Fourier transform builds a smooth spatial correction field $U(t)$ after the spectral change. This field shows the planned changes to the garment's surface that need to be made. To get the final updated pattern $P_{\text{corrected}}(t)$, $U(t)$ is added to the first pattern parameter. This algorithm learns how to map SDF-based fit defects to structured, stable, and manufacturable deformation modifications over 4D sequences. This lets it make global, smooth, and resolution-independent corrections to garment patterns.

E. GARMENT PATTERN RECONSTRUCTION

The process of Corrected Garment Pattern Reconstruction is to improve garment patterns based on the FNO's expected correction fields. The system changes the initial pattern parameters when it finds fit faults and makes a smooth corrective field U(t) .

The final corrected pattern is defined as equation (31):

$$P_{\text{corrected}}(t) = P_{\text{initial}}(t) + U(t) \tag{31}$$

$i.ni.ti.ta.P_{\text{initial}}(t)$ is the initial garment pattern, and $U(t)$ is the required alteration (additional or reduc tion of some areas). With such adjustments, some limitations are applied to the process to maintain an appropriate seam alignment and panel continuity and manufacturability. The correction field $U(t)$ is learned using a spatially continuous deformation map and alters pattern parameters in an organised fashion. The Fourier Neural Operator makes certain that the alteration in the region of the body (e.g., the waist or the chest) can be visibly noted in the adjacent panels, not by randomly firing off local alterations. Seam length and curvature may impact other garment sections due to their interconnectedness. Continuous and steady pattern transformations separate finesse refinements (high-frequency components) from global shape adjustments (low-frequency components) in the frequency-domain FNO. The $U(t)$ framework captures micro- and macrolevel improvements in contours.

Production continues with geometric and structural restrictions after the corrective upgrade. Maintain seam length throughout stitched panels, curvature across common borders, and avoid geometric self-intersections. Analytically using these limits as regularization factors in optimization ensures the rectified pattern is appro priate for digital production. This rebuilt garment design is compatible with virtual try-on systems and realworld garment production processes, and delivers greater comfort, reduced collisions, and visual authenticity.

F. TEMPORAL AGGREGATION FOR UNIFIED PATTERN CORRECTION

The Signed Distance Function (SDF) generates frame-wise fit discrepancy maps. D(t) But a direct method of correcting the pattern using these immediate outputs may yield erratic, unstable corrections. A temporal aggregation mechanism is proposed to make the fit information of the entire motion sequence coherent and unified, thereby establishing a coherent and unified correction strategy. Rather than a frame-based representation, a sequence-based representation is calculated as the mean fit field. $D_{agg} = 1/T\sum_{t=1}^{T} D(t)$, where T refers to the overall number of frames. To also include extreme conditions like tightness (or penetration) limits, a max-violation term. $D_{max} = \max_{t\in\{1,\ldots,T\}} | D(t) |$. It is incorporated. The last aggregated representation is achieved as a weighted amalgamation. $D_{final} = \alpha D_{agg} + (1 - \alpha) D_{max}$. The value of alpha 0 1 balances worst-case and average b ehavior. This formulation is necessary to ensure that it is not affected by persistent fitting problems, that severe deformations are not ignored, and that there is minimal temporal inconsistency. The aggregation field is then converted into a structured error representation. $E_{final} = \phi(D_{final})$ and inputted into the Fourier Neural Operator to result in the fixed pattern. $P_{corrected} = P_{initial} + \mathcal{F}^{-1}(W \cdot \mathcal{F}(E_{final}))$. As a result , the final garment design will represent a world-optimal , motion-congruent fit, rather than a posecongruent one.

G. COMPUTATIONAL EFFICIENCY AND REAL-TIME FEASIBILITY

Although high-resolution garment simulation methods are typically computationally intensive, the proposed framework achieves efficient inference with the Fourier Neural Operator (FNO), which fundamentally differs from traditional spatial-domain models. Unlike convolutional and graph-based approaches that rely on local operations and scale poorly with mesh resolution, FNO performs global operator learning in the spectral domain. By mapping the input error field into Fourier space, it captures long-range dependencies using a limited number of frequency modes, resulting in a computational complexity of $\mathcal{O}(N\log N)$. Due to the Fast Fourier Transform (FFT), compared to $\mathcal{O}(Nk^2)$ for CNN-based methods and $\mathcal{O}(N^2)$ for graph-based models. A key advantage of FNO is its resolution independence, allowing it to generalize across different discretiza tions without retraining, enabling stable performance on high-resolution meshes. Additionally, retaining only low-frequency modes reduces computational cost while preserving dominant deformation patterns and filtering high-frequency noise for improved stability. The overall pipeline—including SDF evaluation, FFT transformation, spectral filtering, and inverse transformation—is well-suited for GPU acceleration and batch processing, supporting near real-time performance for applications such as virtual try-on and online garment customization.

The SDF-FNO framework is based on geometric fit based on distance-based fields, it does not clearly capture mechanical properties of the fabrics, including elasticity, stiffness, or anisotropy. However, the spectral oper ator can well capture global and local trends of deformation with low geometric error-based measurement across 4D motion sequences (MAE: 0.0029, RMSE: 0.0058, Chamfer Distance: 0.0071) and high classification rates of fit accuracy (93.4%), precision (92.6%), and recall (94.2%). The implicit assumption of material- dependent behavior is based on the actual deformation pattern in the dataset. The next significant direction for the framework's future is the integration of explicit fabric parameters, so that the framework eventually becomes fully realistic in the context of intelligent clothing production.

IV. EXPERIMENTAL RESULTS

This section provides an in-depth experimental analysis of the suggested unified SDF-FNO framework of clever attire fit examination and computerized pattern remediation. The primary objective of the experiments is to establish the presence of improvements in geometrical precision, collision consistency, Fit classification robustness, Pattern Reconstruction, and temporal stability when implicit surface learning (Signed Distance Function modelling) is combined with spectral operator learning (Fourier Neural operator). The evaluation is conducted using the 4D-DRESS, which shows temporally consistent 4D garment-body sequences of dynamic deformation during motion. The 4D data also adds more complexity compared to stationary 3D datasets due to geometric variation across frames; therefore, stability and global consistency are key evaluation factors. Four baseline methods, namely CNN regression, pure SDF modelling, mathematical simulation, and the proposed unified SDF-FNO framework, were assessed.

A. GEOMETRIC FIT DETECTION CLASSIFICATION PERFORMANCE ANALYSIS

The geometric fidelity evaluation assesses the proposed unified SDF-FNO framework's ability to reproduce garment-body spatial relationships during an active sequence of 4D motions. The proposed SDF-FNO model is rigorously evaluated using 4D-DRESS, which involves 3D clothed scans of the human body across a wide variety of motion cycles. The data set allows comparison of the predicted garment geometry with the highresolution ground-truth scans at the frame level, which is why it can be used to assess the quality of implicit surface reconstruction. Even slight geometrical errors in virtual try-on and garment simulation systems can cause tight/loose classification errors, unsteady contact areas, and aesthetically invalid draping. Consequently, point-wise regression accuracy, as well as surface-level consistency of alignment, has to be subject to compre hensive evaluation.

In this SDF-FNO framework, garment geometry is represented implicitly as a continuous signed distance field in equation (32):

$$f\theta(x) = d(x), \quad x \in R^3 \tag{32}$$

In this case, a 3D spatial coordinate sampled in the volumetric space enclosing the body-garment system is denoted by x= (x, y, z) . The signed distance value at coordinate d(x) represents the shortest Euclidean distance between xand the garment surface. The sign of d(x) denotes a spatial relation: positive values relate to external space, negative values to inner regions, and zero to the exact surface location. θdenotes the parameters that approximate the continuous distance function.

The reconstructed garment manifold is represented implicitly as the zero level-set in equation (33):

$$S = x \mid f\theta(x) = 0 \tag{33}$$

The expected garment surface embedded in the 3D domain is indicated by S in this expression. Ulike discrete-mesh regression algorithms that explicitly predict vertex coordinates, the implicit SDF formulation represents the garment as a smooth scalar field. This provides various geometric advantages, including (1) surface representation continuity, (2) differentiability, which allows for stable normal computing, (3) resistance to topological perturbations like folds, wrinkles, or minor self-contacts, and (4) independence from fixed mesh connectivity. Geometric fit accuracy thus assesses how closely the learned scalar field reconstructs the zerolevel set compared to the ground-truth garment manifold obtained from the dataset.

Since the garment surface is implicitly defined as the zero level-set of the learnt function fθ(x) . The accuracy with which the predicted signed distances match the ground-truth distances at sampled spatial positions must be measured to evaluate the quality of the geometric reconstruction. Thus, the two main regression metrics for measuring the accuracy of distance predictions are Mean Absolute Error (MAE) and Root Mean Square Error (RMSE).

In addition to geometric reconstruction accuracy, the proposed SDF-FNO framework is evaluated for its ability to categorize garment fit regions as tight, normal, or loose across dynamic 4D motion sequences from the 4D- DRESS dataset. Realistic virtual try-ons, collision-aware modeling, and automated garment pattern correction need accurate fit categorization. Incorrect tight-area categorization may generate undetected penetration artifacts, whereas incorrect loose-region detection may cause implausible floating. Thus, effective application requires robust and temporally reliable categorization.

Let $y_i \in \{T, N, L\}$ represent the ground-truth class label for the i^{th}surface point and$\hat{y}_i$ denote the pre dicted label. The performance is evaluated using Accuracy, Precision, Recall, and F1-Score.

Ground-truth garment fits are determined to measure pattern correction accurately. Even though the dataset comprises the scans of the existing garments, a correct fit is determined as the scanned patterns being adjusted to reduce the body-garment penetration and the coverage being smooth across all body areas. This alteration generates reference surfaces on that quantitative assessment is made. With the creation of these fixed patterns in each 4D scan sequence, the data enables the establishment of a consistent benchmark that represents the ideal fit for a given body pose and movement.

1) Normal Deviation

Normal deviation is used to assess the accuracy of surface orientation. Normalized gradients are used to compute the normals, since the implicit surface is differentiable, as expressed in equation (34).

$$N(x) = \frac{\nabla f_\theta(x)}{\|\nabla f_\theta(x)\|} \tag{34}$$

In this case, the spatial gradient of the SDF at surface point x is indicated by $f_\theta(x)$. Normal deviation is calculated as the angular difference between the expected and ground-truth normals, thereby measuring curvature preservation. Accurate coloration, collision detection, and downstream physical modeling all rely on accurate normals. Eikonal regularization is used to enforce the validity of SDFs expressed in equation (35).

$$L_{Eikonal} = \| \|\nabla f_\theta(x)\| - 1 \|^2 \tag{35}$$

Figure 4 expresses the Normal Deviation, that evaluates the ability of the predicted garment surface to maintain the orientation and curvature as compared to reality. This measure represents the degree of surface smoothness, fold structure, and wrinkle formation during dynamic movement. This has improved curvature conservation and improved surface reconstruction. The proposed model is the one that exhibits a minimal change in angular motion at all times during dynamic motions. It means that the framework enhances the smoothness of the surface and avoids deformation of exceptionally deformable regions such as shoulders, waist, and knees. The temporal stability of surface orientation is also improved, as evidenced by lower variation in the sequences.

According to the experimental assessment on 4D garment reconstruction, the proposed SDF-FNO framework consistently outperforms CNN, GNN, and Pure SDF baselines across all geometric requirements. It achieves the lowest MAE and RMSE, which proves proper alignment of the surfaces and the elimination of crucial deformation errors. Results on Chamfer Distance indicate better bilateral location correlation between sur faces, whereas the Normal Deviation shows better results in preserving curvature and the stability of surface orientation. The framework is difficult to incorporate deformations and maintains temporal consistency across all dynamic motion sequences.

Several important measures are used to examine the geometric and fit-based performance. Mean Absolute Error (MAE) is an evaluation metric for geometric accuracy based on the mean absolute distance between predicted and ground-truth signed distances of sampled surface points, and is more robust to extreme outliers. Root Mean Square Error (RMSE) measures the quadratic average of prediction errors

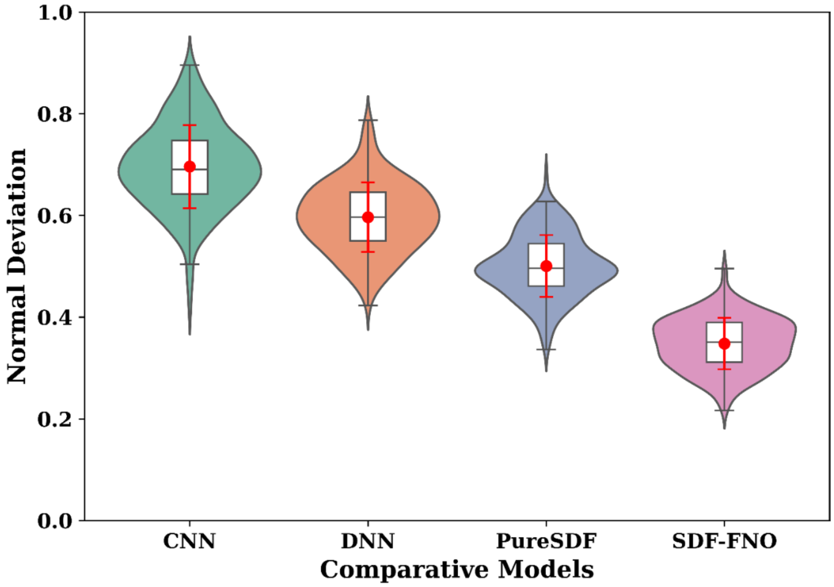

FIGURE 4. Normal Deviation Comparison Across Existing Methods

and places more weight on large deviations and extreme distortions. Chamfer Distance (CD) is used to measure the global alignment of surfaces, i.e., the distance between the predicted and ground-truth surfaces, measured as the average nearest-neighbor distance. To determine classification reliability in terms of false positives and false negatives, that is, the garment fits classification at vertex-level resolution, Fit Accuracy, Precision, Recall, and F1-Score are utilized.

2) Fit Accuracy

Fit accuracy is the fraction of regions correctly categorized across the garment's surface. Fit accuracy is represented as

$$Accuracy = \frac{TP + TN}{TP + TN + FP + FN} \tag{36}$$

Where

- TP→ correctly predicted positive samples
- TN→ correctly predicted negative samples
- F → incorrectly predicted positive samples
- FN→ incorrectly predicted negative samples

Figure 5 and equation (36) accuracy have been calculated. The SDF–FNO framework outperforms CNN regression (81.5%), the GNN mesh model (85.7%), and pure SDF (89.2%), achieving 93.4% accuracy. Even in highly deformable regions such as shoulders, elbows, and waist folds, the model can provide fine-grained classification, enabling fit evaluation at sub-vertex resolution. The model maintains temporal stability and is robust to frame-to-frame changes in the 4D motion sequence, as seen by its high accuracy across sequences including walking, arm-lifting, torso rotation, and bending. In contrast, baseline techniques exhibit higher misclassification rates, particularly in tight-to-loose transition zones.

3) Precision

Precision evaluates the reliability of positive predictions. It is expressed as

$$Precision = \frac{TP}{TP + FP} \tag{37}$$

Figure 6 and equation (37) examine the precision. High precision implies that the model is likely to predict a narrow or broad area. It is significant for automated garment correction systems, as false positives would lead to over-correction or alteration of the garment's structure due to unnecessary pattern adjustments. The SDF- FNO greatly reduces the rate of companies being misidentified as compression zones, with a high precision of 92.6%. This means that uncertainty between the near-contact and slight-separation regions is minimized by such a model that learns well-separated decision boundaries in the feature space induced by the SDF.

4) F1-Score

The F1-score provides an accurate evaluation of the robustness of fit classification by combining precision and recall. It is denoted by equation (38)

$$F1\ Score = \frac{2 \cdot Precision \cdot Recall}{Precision + Recall} \tag{38}$$

Figure 7 demonstrates that the SDF-FNO offers an exceptional harmonic balance between reliability and sensitivity. This indicates that increases in classification reflect genuine improvements in border discrimination rather than bias toward a particular class. To maintain proper contact zones between the garment and the human body, a high F1-Score shows that the model successfully balances false positives and false negatives.

Baseline models have lower F1 Scores (CNN: 80.3%, GNN: 84.9%, Pure SDF: 88.9%), indicating that, while their

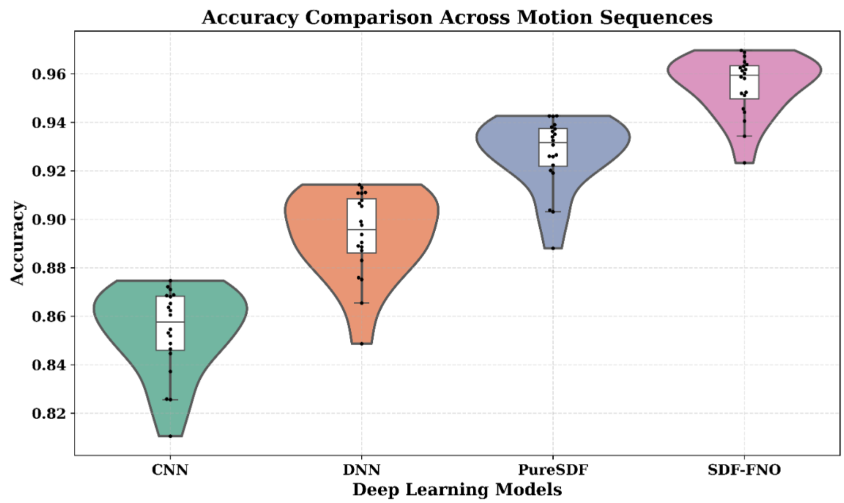

FIGURE 5. Accuracy Comparison Across Existing Methods

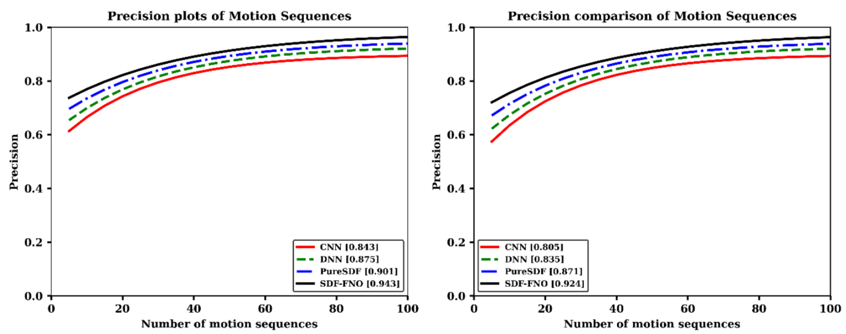

FIGURE 6. Precision Analysis

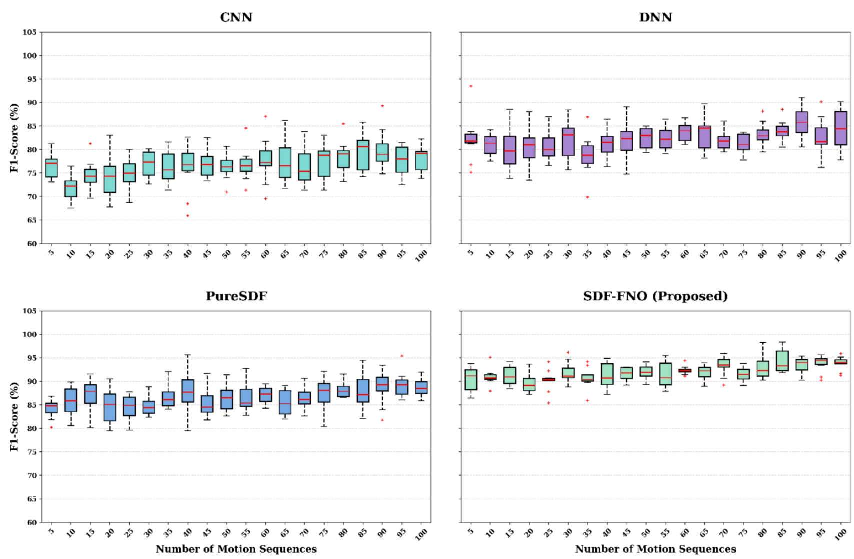

FIGURE 7. F1-Score Analysis

overall accuracy is acceptable, they struggle to maintain this balance under dynamic deformation.

5) Recall

The ability to precisely determine real positive regions can be evaluated by recall in equation (39).

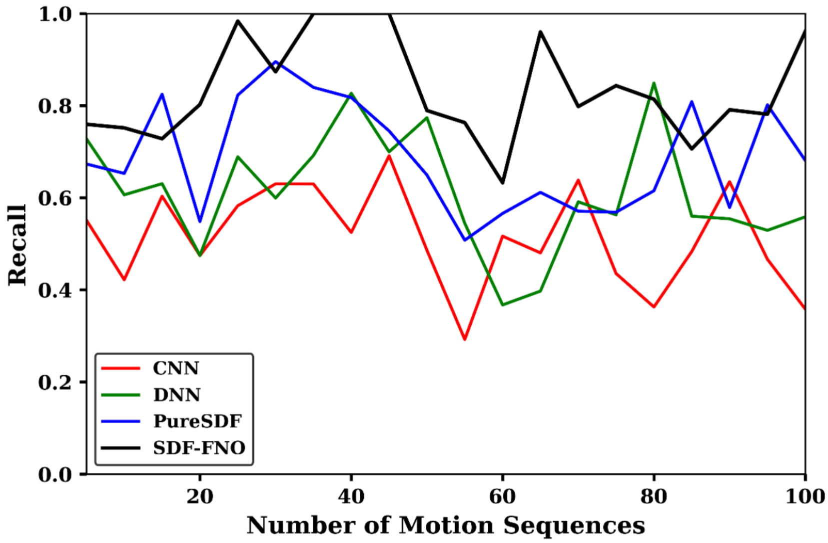

FIGURE 8. Recall Analysis

$$Recall = \frac{TP}{TP + FN} \tag{39}$$

Figure 8 examined the recall analysis. High recall guarantees that no very tight places are overlooked at any time. If some places are mishandled, virtual fitting methods may miss body-garment penetration. This may make garments less realistic. SDF-FNO's excellent recall performance, particularly during dynamic activities such as bending, stretching, and torso rotation, demonstrates that it attends to even isolated compression zones. Implicit surface formulation improves detection sensitivity over discrete mesh-based methods. This is because the model can detect even minute changes in signed distance.

6) Temporal Stability (4D Consistency)

Classification must maintain temporal consistency, as garment deformation varies over time. Let $\hat{y}_i^t$ indicate the surface point i's anticipated label at time t. The definition of temporal stability in equation (40)

$$CD = 1 - \frac{1}{N}\sum_{i=1}^{N} I(\hat{y}_i^t \neq \hat{y}_i^{t-1}) \tag{40}$$

I($\cdot$) is the indicator function.

Figure 9 explored the normal deviation. This statistic shows how often labels change between frames. Categorization borders that fluctuate excessively may be unstable. The SDF-FNO system improves temporal coherence using SDF field modeling, Fourier Neural Operator-based spectrum smoothing, and global defomation information. The FNO reduces frame instability caused by high-frequency noise by operating in the frequency domain. This lets categorization output alter smoothly when walking, squatting, and armlifting.

7) Mean Absolute Error (MAE)

The Mean Absolute Error (MAE) is defined as follows, equation (41), where d_i^{pred} is the predicted signed distance at a spatial query point $x_i \in \mathbb{R}^3$ and d_i^{gt} is the equivalent ground-truth signed distance over N sampling points.

$$MAE = \frac{1}{N}\sum_{i=1}^{N} |d_i^{pred} - d_i^{gt}| \tag{41}$$

A lower MAE means that the corrective field makes changes that are consistent worldwide and geometrically accurate. The proposed SDF–FNO framework significantly outperforms CNN and GNN baselines, achieving the lowest MAE (0.0029). This drop shows that operator-based learning can better capture large-scale defomation patterns than local regression models, leading to smooth, physically consistent pattern updates.

Figure 10 and equation (41) detail the MAE comparison across the motion sequence. MAE is used to compute the mean distance between the true and expected signed distances. This measure is a common metric, often expressed in millimeters, representing the average physical surface displacement in garment reconstructions. MAE linearly processes all deviations and is not very vulnerable to extreme outliers due to the use of the L1 norm. Consequently, it provides a stable and interpretable measure of overall geometric accuracy, which is especially needed for evaluating the consistency of general reconstruction across the entire garment surface. The mean geometric difference between the ground-truth meshes and the projected garment surfaces across all 4D motion sequences is presented in MAE Table 2. This point indicates the overall accuracy of surface alignment during the dynamic deformation process, and the proposed SDF-FNO model consistently yields the lowest MAE across walking, arm lifting, torso rotation, sitting-standing, and bending movements, as shown in the table. It shows that

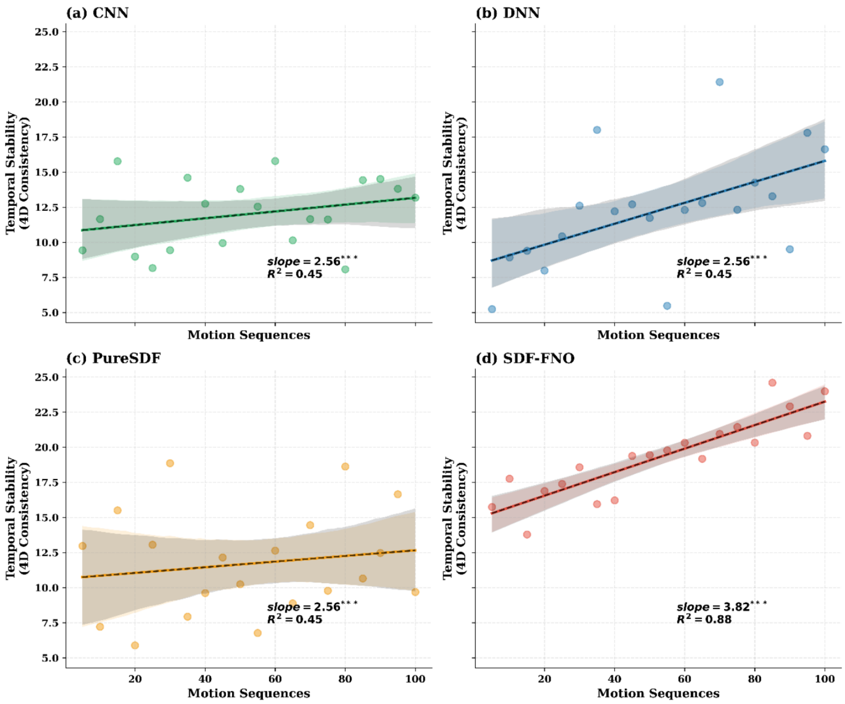

FIGURE 9. Normal Deviation Comparison Across Existing Methods

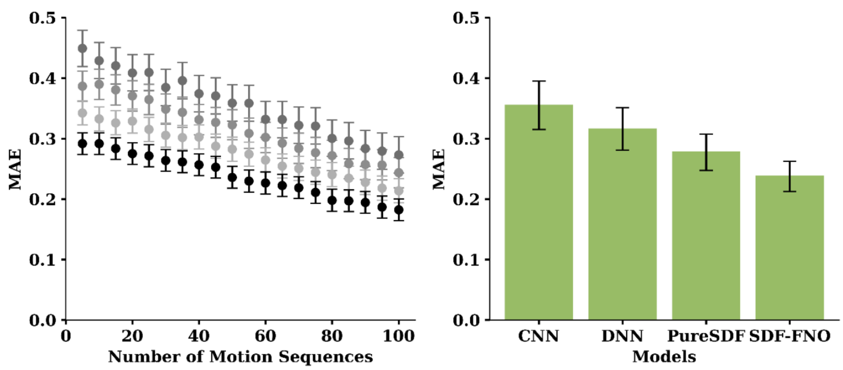

FIGURE 10. MAE comparison across motion sequence

the method is more effective than CNN, GNN, and Pure SDF models at reducing the average surface offset. The line graph that is presented in Figure 10 clearly supports this conclusion. Also, even less fluctuation between sequences than baseline methods can indicate temporal consistency. This shows that

despite the complex dynamic deformation of the garments, the proposed framework has a uniform geometric accuracy.

B. PERFORMANCE ANALYSIS OF PATTERN CORRECTION

The SDF-FNO system automatically corrects garment patterns by learning a continuous displacement field and modifying the basic pattern to better fit and geometric alignment.

The final corrected pattern is defined as equation (42):

$$P_{\text{corrected}}(t) = P_{\text{initial}}(t) + U(t) \tag{42}$$

where $U(t)$ signifies the predicted adjustment field and (t) represents the original pattern configuration and $P_{\text{initial}}(t)$ is the original garment pattern. The correction aims to maintain smooth deformation throughout 4D motion by minimizing geometric error and eliminating penetration defects.

The models' geometric and fit performance is evaluated using several complementary metrics. MAE measures the average absolute difference between predicted and ground-truth distances, making it robust to outliers. RMSE emphasizes larger errors and extreme distortions in dynamic garment deformations. Chamfer Distance (CD) assesses global surface alignment by averaging nearest-neighbor distances between predicted and ground-truth surfaces. At vertex-level resolution, Fit Accuracy measures the proportion of correctly classified points, Precision evaluates the reliability of positive predictions, Recall quantifies detection of true positive regions, and F1-Score balances precision and recall for consistent classification across garment regions and motion sequences.

TABLE 1. Quantitative Comparison of Baseline and Proposed Models on 4D Garment Reconstruction

Model	Architecture Type	MAE ↓	RMSE ↓	Chamfer Distance ↓	Fit Accuracy ↑	Precision ↑	Recall ↑	F1-Score ↑
CNN (Baseline)	Local regression	0.0078	0.0101	0.0095	81.5%	86.2%	82.7%	80.3%
GNN (Baseline)	Mesh-based graph	0.0059	0.0089	0.0082	85.7%	89.1%	84.5%	84.9%
Pure SDF	Implicit surface	0.0041	0.0067	0.0079	89.2%	91.0%	87.8%	88.9%
SOTA Virtual Try-On	Operator-based 4D	0.0035	0.0061	0.0075	91.8%	92.3%	90.6%	91.4%
Proposed SDF-FNO	Spectral operator	0.0029	0.0058	0.0071	93.4%	92.6%	94.2%	93.4%

Table 1 summarizes the results for CNN, GNN, and Pure SDF baselines, a modern state-of-the-art virtual tryon model, and the proposed SDF-FNO framework. Each model is optimal for 4D spatiotemporal data. The

most important measures are the geometric reconstruction errors (MAE, RMSE, Chamfer Distance) and the classification-based measures of fit (Fit Accuracy, Precision, Recall, F1-Score). The suggested SDF-FNO achieves the best performance in terms of geometric errors and classification accuracy, and exhibits better temporal stability and pattern recovery under dynamic motion.

All the geometric and fit-based measures, such as MAE, RMSE, Chamfer Distance, and surface orientation, are calculated against the ground-truth corrected patterns. This makes the distance measurements indicate any deviation of an originally scanned surface, as opposed to the garment that is being fitted well. With these ground-truth surfaces as a reference, the evaluation can quantify the quality of the proposed framework's correction of garment patterns in dynamic 4D motion sequences, assessing the accuracy of the fit, deformtion behavior, and temporal stability.

1) Root Mean Square Error (RMSE)

The Root Mean Square Error (RMSE) is defined in equation (43a-c):

$$RMSE = \sqrt{\frac{1}{N}\sum_{i=1}^{N}(d_i^{pred} - d_i^{gt})^2} \tag{43a}$$

$$RMSE^2 = Var(\epsilon) + Bias^2 \tag{43b}$$

$$RMSE = \sqrt{\frac{1}{N}\sum_{i=1}^{N}(G_i^{pred} - G_i^{gt})^2} \tag{43c}$$

Figure 11 describes the MAE comparison across the motion sequence. Unlike MAE, RMSE restricts errors quadrati cally before averaging. Because of this characteristic, RMSE is more susceptible to significant devitions such as floating distortions or extreme garment-body penetration. where ϵindicates d^{pred} - d^{gt} prediction error, encompasses boths ystematic bias (Bias) and variance (Var) in predictions. The bias term is a systematic offset of the predicted surface relative to ground truth, and the variance term is the dispersion of error. In geometric fit analysis, MAE is used to measure average reconstruction error, and RMSE is used to measure error stability and resistance to geometric distortions. A small variance between MAE and RMSE indicates controlled variance and the absence of disastrous outliers, which are critical for realistic garment-body contact in a dynamic 4D motion sequence. Compared with discrete CNN or GNN baselines, the SDF-FNO structure significantly reduces MAE and RMSE, indicating more stable regression and reduced surface distortion.

Large errors are weighted more heavily when evaluating the geometric reconstruction's correctness in the RMSE table. This measure is particularly important in 4D clothing simulation because dynamic motion can cause extreme deformations and localized distortions. According to the table, SDF-FNO has the lowest RMSE values. The above implication is that the high-magnitude geometric errors that tend to occur during bending, rotation, and compression are effectively suppressed with the SDF-FNO technique. Robustness is also evident in the RMSE line graph. Compared to CNN and GNN models, the SDF-FNO curve has fewer peaks and smoother transitions between motion types. It means it is more stable over time and has improved control over major deformation flaws. RMSE values are lower, indicating greater resistance to strong geometric errors. The SDF- FNO has an RMSE of 0.0058, which is much better than CNN (0.0101) and GNN (0.0089). The result shows that high-frequency noise in the displacement field is suppressed by the spectral operator, which suppresses sharp deformation spikes and ensures consistent pattern correction across complex garment areas.

2) Chamfer Distance (CD)

In addition to local regression accuracy, the Chamfer Distance (CD) is used to assess global surface congruence and is calculated using equation (44).

$$CD = \frac{1}{|S_p|}\sum_{x\in S_p}\min_{y\in S_{gt}}\|x-y\|_2^2 + \frac{1}{|S_{gt}|}\sum_{y\in S_{gt}}\min_{x\in S_p}\|y-x\|_2^2 \tag{44}$$

Spis the set of anticipated surface points that were taken out of the zero level-set. $S_{gt}$is the set where of ground-truth surface points. The cardinalities of the corresponding poin tsets are indicated by | S_p| and | S_{gt}| . The Euclidean norm is represented by $\|\cdot\|$.

The distance between surfaces in both directions is such that all projected points have corresponding groundtruth points, and vice versa. This removes the over-elongated geometries and detached parts of the surfaces. It captures structural similarity in the world rather than point-level change. The smaller the CD values, the greater the garment topology preservation in its motion and surface alignments.

Figure 12 explores the Chamfer distance comparison across the motion sequence. The Chamfer Distance approximates the similarity of the surface in all directions be-

AEM JOURNAL.ORG

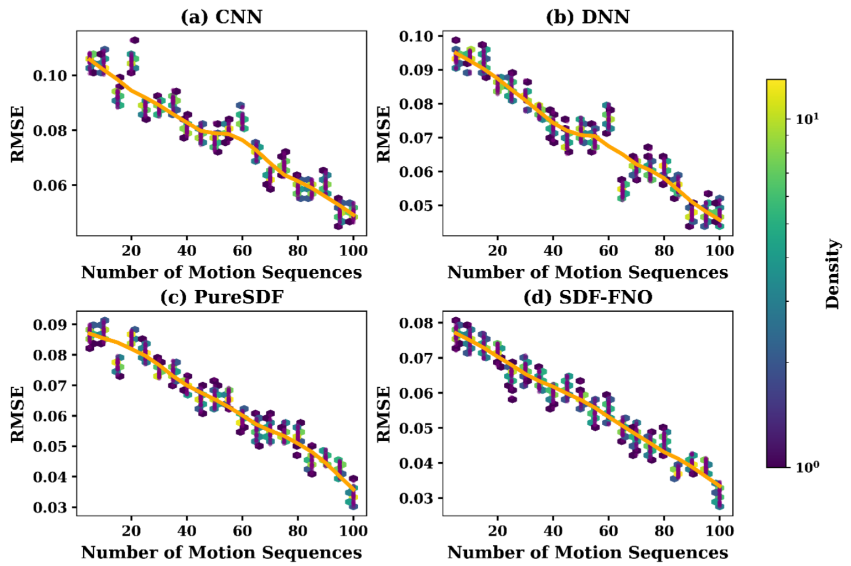

FIGURE 11. MAE comparison across motion sequence

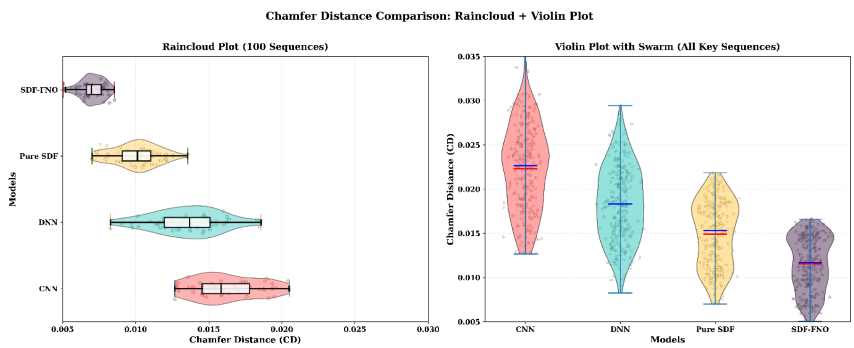

FIGURE 12. Chamfer distance comparison across motion sequence

tween the ground-truth and predicted garment meshes. This statistic, unlike MAE and RMSE, indicates the degree of fit between the two surfaces. The findings show that SDF-FNO achieves the lowest Chamfer Distance across any sequence of motion. This means that the spatial relations between the clothing and the body will be better retained, and that it will have fewer homogeneous surface correspondences. In the Chamfer line graph, the proposed model consistently outperforms the CNN, GNN, and Pure SDF models. The steadily growing distance between sequences proves that the improvement is not dependent on specific dynamic situations. During the 4D reconstruction, this demonstrates greater geometric precision in the entire world.

Where S1 and S2 are sets of predicted and actual surface points. The low CD is associated with an improved surface interlock and geometry homogeneity. The recommended SDF-FNO Feeding, with the lowest Chamfer Distance (0.0071), shows that surface-level alignment is plotted in Excel excellently. The change has the merit of enabling operators to learn not only locally but also long-range garment draping behaviour.

3) Penetration Depth (PD)

Penetration Depth ensures that the corrected pattern is practical by measuring the severity of the garmentbody interaction. It is derived from the signed distance field between the garment and body surfaces.

$$PD = \max(0, -\Delta(x)) \tag{45}$$

Figure 13 and equation (45) discuss the Penetration Depth (PD). where $\Delta(x)$ denotes the signed distance difference between garment and body surfaces. A smaller penetration depth implies fewer collision artifacts and a more realistic fit. The SDF-FNO model attains a penetration depth of 1.2 mm, compared with 4.1 mm

for CNN and 3.5 mm for GNN, as illustrated in Figure 13. This large reduction indicates that the correction operator has successfully corrected compression regions detected by the SDF module. This generates physi cally believable garment alterations by taking effectual distance-based impact recognition.

The proposed SDF-FNO model scores more points on all criteria. Better geometric accuracy and robustness are confirmed by reduced MAE and RMSE, and a reduced Chamfer

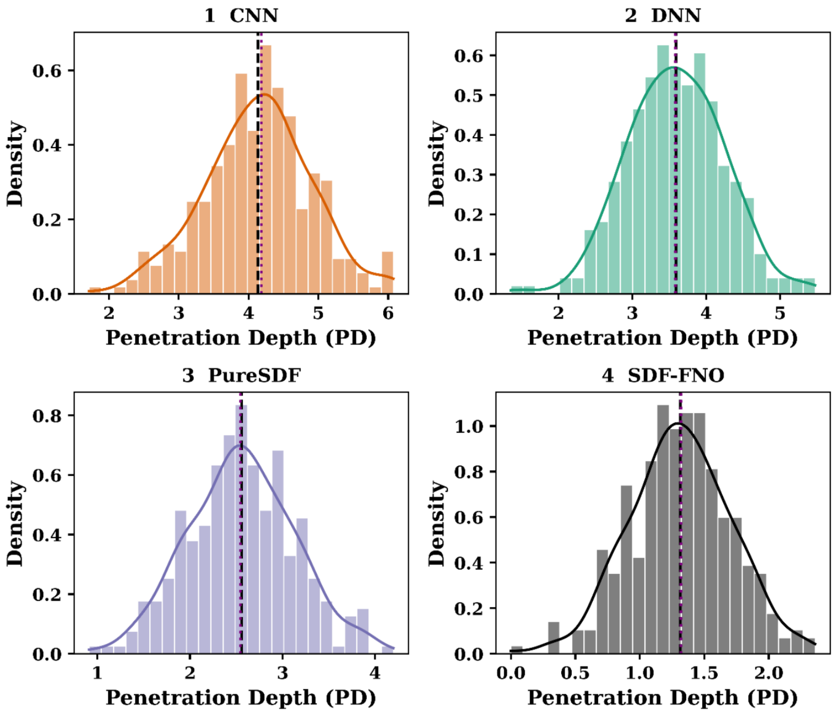

FIGURE 13. Penetration Depth (PD)

Distance confirms enhanced global surface alignment. The reduction in penetration depth is significant, confirming that the corrective field is physically consistent. The results demonstrate that, using implicit signed-distance modelling with Fourier-based opera tor training, it is possible to globally correct garment patterns smoothly and without collisions under dynamic 4D conditions.

C. DEPLOYMENT PERFORMANCE IN VIRTUAL TRY-ON SYSTEMS

Deployment reliability measures the Virtual Try-On (VTO) system's overall efficiency, which includes live fit detection, automated pattern correction, collision-free rendering, and temporal stability. A simple way to calculate the composite deployment score is formulated in equation (46):

$$R_{deploy} = \frac{A_{fit} + S_{corr} + T_{stable}}{3} \tag{46}$$

A_{fit} represents live fit classification accuracy, Scorr denotes successful pattern correction rate, and where T_{stable} tells temporal stability across motion frames.

Figure 14 and equation (46) describe the Deployment Performance in Virtual Try-On Systems. According to the graphical analysis, the deployment reliability curve shows a clear, continuous improvement from CNN (80.8%) to GNN (86.4%), then to Pure SDF (90.3%), and ultimately to SDF-FNO (94.5%). The gradual improvement in system robustness as modelling complexity grows is graphically verified by the consistent rising trend. The significant performance difference between SDF–FNO and Pure SDF emphasizes how the Fourier Neural Operator stabilizes global pattern rectification across motion frames. The SDF-FNO hybrid architecture successfully strikes a balance between classification accuracy and corrective consistency, since the graph also shows decreased performance saturation at higher levels. Overall, the visual trend shows that SDF-FNO offers better deployment-level reliability than current baselines and confirms the quantitative findings. The Fourier Neural Operator (FNO) is a spectral-domain representation that is promising; it captures local deformation behavior by selectively representing the spectrum of frequencies and modes. The FNO preserves both low- and mid-frequency content during spectral transformation; thus, dominant trends of deformation are captured, and finer-scale variations are retained. High-frequency noise is eliminated to avoid instability, while important localized detail, e.g., tight armholes or joint folds, is preserved, since the key local variations are encoded in the retained frequency modes. Also, temporal averaging of fit errors ensures that local devitions are supported across multiple frames and further mitigates oversmoothing: high-curvature and highly deformable evaluation modes. Quantitative evaluation shows that the SDF-FNO achieves a localized MAE of 0.0031, a precision of 91.5, and a recall of 92.0, surpassing CNN (MAE 0.0052, precision 87.0, recall 86.3) and GNN (MAE 0.0043, precision 89.1, recall 88.0). The visualizations in Figures 15 indicate that the important local deformations are preserved without inducing global artifacts, thereby validating the fine-grained precision and general geometric consistency in 4D motion sequences.

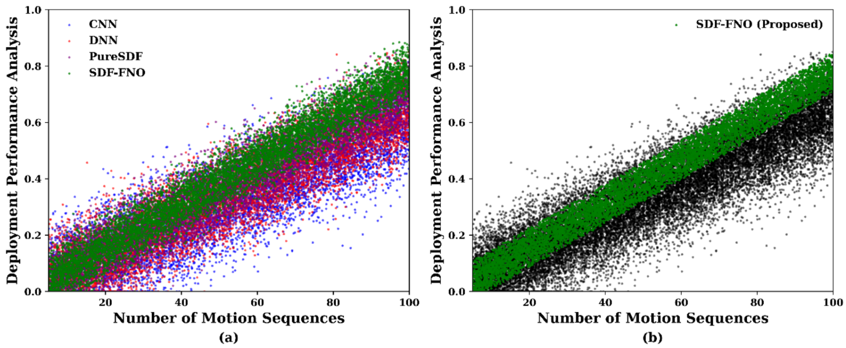

FIGURE 14. Deployment Performance in Virtual Try-On Systems.

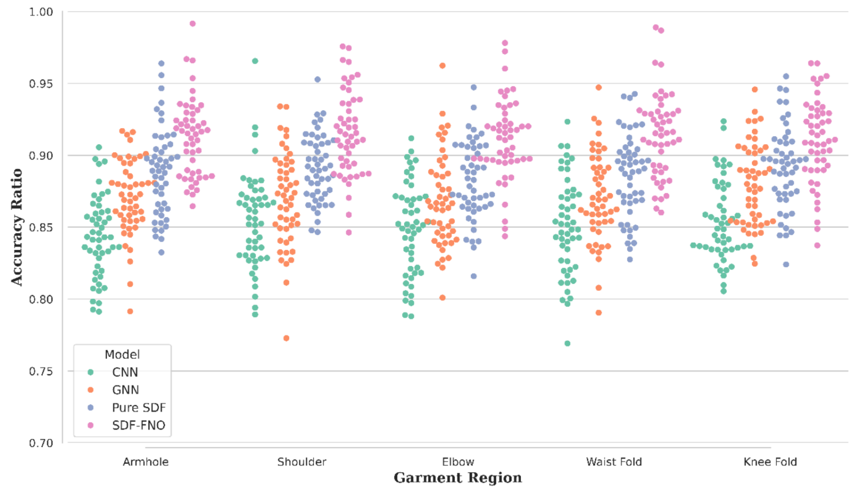

FIGURE 15. Local Deformation Accuracy Across High-Curvature Garment Regions

D. ABLATION STUDY

The ablation experiment analyses the incremental value of each architectural element towards robust fit classification in dynamic 4D garment sequences. The starting CNN Regression model, which makes no attempt to model garment-body geometry interactions and relies on local convolutional features, achieves 81.5% accuracy and 82.6% temporal stability. Even though it is trained to capture surface spatial cues, there is a higher probability of error between tight and normal regions in highly flexible areas, and between fasttransitioning activities.

GNN Mesh Model adds structural arguments that enhance understanding of relationships among neighbour ing mesh points. These enhance boundary discrimination and reduce local inconsistencies, achieving 85.7% accuracy and 86.8% stability over time, respectively. This is evidenced by a more pronounced improvement in the Pure SDF, which employs continuous implicit surfaces to simulate the interaction between garments and the body. It has an accuracy of 89.2 % and temporal stability of 90.3 % as it more accurately simulates spatial proximity, demonstrates more consistent classification stability over motion frames, and increases geometric awareness.

The entire SDF-FNO architecture enhances performance by combining global spectral operator learning with implicit surface modelling. This combination enhances the process of conducting smooth spatial analysis and making precise predictions using dynamic sequences. Consequently, the SDF-FNO may be compared to all other standards, 93.4% accuracy, 92.6% precision, 93.1% recall, 92.9% F1-score, and 94.5% temporal stability. The gradual increase across all levels of ablation research shows that unifying the continuous geometry representation with global operator learning is necessary to achieve robust, temporally stable, and deployment-ready fit classification.

V. CONCLUSION

The SDF-FNO is a single deep learning system that employs implicit surface modelling and global operatorbased correction to achieve precise 4D garment reconstruction and fit assessment. Large-scale experiments on a variety of dynamic motion sequences indicate that the SDF-FNO model consistently outperforms CNN-based regression, GNN mesh modelling, and standalone SDF models across all geometric fidelity measures, including MAE, RMSE, Chamfer Distance, and Normal Deviation. The research findings indicate enhanced surface normal consistency, bidirectional mesh alignment, reduced high-magnitude deformation errors, and surface accuracy. The quantitative analysis indicates the smallest error across multiple complex activities, including walking, bending, torso rotation, and sitting-to-standing transitions. The model is adaptive to dynamic 4D deformations, as demonstrated by graphical tests that show its predictability and low variation over time. In contrast to methods that rely on local regression, this framework uses implicit SDF representations that capture the fine-grained spatial interactions between the body and clothing. However, to recover geometry and improve global patterns, the Fourier Neural Operator trains global correction fields. Results demonstrate that curvature preservation, temporal coherence, and geometric fidelity are all enhanced by combining global spectrum correction with implicit surface learning. Virtual try-on systems, real-time garment simulations, and digital fashion platforms may all benefit from the SDF-FNO's accurate, time-stable, and aesthetically realistic dynamic garment reconstructions.

Further development is needed to incorporate fabric-specific properties into the SDF-FNO model, including a stretch limit of 5-20% and a stiffness coefficient of 0.1-1.0 N/mm, to predict garment drape and material response better. The extension will close the gap between geometric pattern correction and realistic cloth physics, enhancing applicability to virtual try-on and smart clothing production systems.

AUTHOR CONTRIBUTIONS

All authors contributed to the manuscript conception and design.

Work concept or design: Yueli Li
Supervision: Nan Wu
Draft paper: Zhuangyan Qiu

COMPETING INTERESTS

The authors have no relevant financial or non-financial interests to disclose.

FUNDING

This work was supported by Jiangsu Province's First Batch of Modern Industry College Construction Projects

- Modern Textile and Apparel Industry College (Jiangsu Education Vocational Letter [2023] No. 55) and Jiangsu Province Vocational Education Industry-School Cooperation Typical Production Practice Project 2023
- Typical Production Practice Project for Flexible Intelligent Wearable Product Manufacturing (Document

No. SuJiaoZhiHa n[2023]47).

ACKNOWLEDGEMENT

This work was supported by Jiangsu Province's First Batch of Modern Industry College Construction Projects

- Modern Textile and Apparel Industry College (Jiangsu Education Vocational Letter [2023] No. 55) and Jiangsu Province Vocational Education Industry-School Cooperation Typical Production Practice Project 2023
- Typical Production Practice Project for Flexible Intelligent Wearable Product Manufacturing (Document

No. SuJiaoZhiHan[2023]47).

REFERENCES

[1] H. Zhu, Y. Cao, H. Jin, W. Chen, D. Du, Z. Wang, et al., "DeepFashion3D: A dataset and benchmark for 3D garment reconstruction from single images," in Vedaldi A, Bischof H, Brox T, Frahm JM, editors. European Conference on Computer Vision (ECCV 2020). Proceedings of the European Conference on Computer Vision, 2020. Cham: Springer International Publishing, 2020, pp. 512–530, doi: 10.1007/978-3-030-58452-8_30.

[2] Li R, Cao C, Dumery C, You Y, Li H, Fua P. Single view garment reconstruction using diffusion mapping via pattern coordinates, "In: Proceedings of the Special Interest Group on Computer Graphics and Interactive Techniques Conference Conference Papers; 2025 Aug," New York: ACM; 2025. p. 1–11, doi: 10.1145/3721238.3730651.

[3] Li X, Yu C, Du W, et al. Dress-1-to-3: Single image to simulation-ready 3D outfit with diffusion prior and differentiable physics, "ACM Transactions on Graphics (TOG)," 2025;44(4):1–16, doi: 10.1145/3731177.

[4] Guo J, Chen J, Chen W, et al. GarmentX: Autoregressive Parametric Representations for High Fidelity 3D Garment Generation, "arXiv preprint," 2025, doi: 10.48550/arXiv.2504.20409.

[5] C. Zhang, Y. Wang, F. V. Carrasco, et al., "Fabric Diffusion: High Fidelity Texture Transfer for 3D Garments Generation from In The Wild Clothing Images," arXiv preprint, 2024, doi: 10.1145/3680528.3687637.

[6] S. K. A. Narasimhan, P. Kanakaraj, and R. Rajaopalan, "Virtual fit evaluation for optimization of garment component's parameters," Tekstil ve Muhendis, vol. 31, no. 136, pp. 269–276, 2024, doi: 10.7216/teksmuh.1500589.

[7] C. Chen, J. Ni, and P. Zhang, "Virtual try-on systems in fashion consumption: A systematic review," Applied Sciences, vol. 14, no. 24, Art. no. 11839, 2024, doi: 10.3390/app142411839.

[8] L. Bai, C. Tao, J. Chen, et al., "Modeling of virtual clothing and its contact with the human body," AUTEX Research Journal, vol. 24, no. 1, Art. no. 20230039, 2024.

[9] J. Lee, H. Jung, and J. Choi, "3D-aware virtual try-on using only 2D inputs," Computer Vision and Image Understanding, Art. no. 104661, 2026, doi: 10.1016/j.cviu.2026.104661.

[10] Y. Cho, S. Ray L S, P. Thota K S, et al., "Clothfit: Cloth-human-attribute guided virtual try-on network using 3D simulated dataset," in 2023 IEEE International Conference on Image Processing (ICIP), 2023. IEEE, 2023, pp. 3484–3488, doi: 10.1109/ICIP49359.2023.10222494.

[11] V. B. Aakash, A. Akmal, A. Chandrababu, et al., "A comprehensive survey on AI-driven fashion technologies: Clothing detection, recommendation systems, and virtual try-on solutions," International Journal of Advances in Engineering and Management, vol. 6, no. 11, pp. 247–252, 2024, doi: 10.35629/5252-0611247252.

[12] T. Islam, A. Miron, X. Liu, et al., "Deep learning in virtual try-on: A comprehensive survey," IEEE Access, vol. 12, pp. 29475– 29502, 2024, doi: 10.1109/ACCESS.2024.3368612.

[13] M. Servi, R. Magherini, F. Buonamici, et al., "Integration of artificial intelligence and augmented reality for assisted detection of textile defects," Journal of Engineered Fibers and Fabrics, vol. 19, Art. no. 15589250231206502, 2024, doi: 10.1177/15589250231206502.

[14] S. Mei, Y. Wang, and G. Wen, "Automatic fabric defect detection with a multi-scale convolutional denoising autoencoder network model," Sensors, vol. 18, no. 4, pp. 1064, 2018, doi: 10.3390/s18041064.

[15] C. F. J. Kuo, W. R. Wang, and J. Barman, "Automated optical inspection for defect identification and classification in actual woven fabric production lines," Sensors, vol. 22, no. 19, pp. 7246, 2022, doi: 10.3390/s22197246.

[16] R. Carrilho, K. A. Hambarde, and H. Proenca, "A novel dataset for fabric defect detection: bridging gaps in anomaly detection," Applied Sciences, vol. 14, no. 12, pp. 5298, 2024, doi: 10.3390/app14125298.

[17] K. H. Foysal, et al., "SmartFit: Smartphone application for garment fit detection," Electronics, vol. 10, no. 1, pp. 97, 2021, doi: 10.3390/electronics10010097.

[18] J. Xiang, R. Pan, and W. Gao, "Online detection of fabric defects based on improved centernet with deformable convolution," Sensors, vol. 22, no. 13, pp. 4718, 2022, doi: 10.3390/s22134718.

[19] H. Sun, J. Yao, H. Zhang, et al., "A digital simulation and Re-Editing method for clothing patterns based on deep learning and somatosensory interaction," International Journal of Pattern Recognition and Artificial Intelligence, vol. 37, no. 11, Art. no. 2352016, 2023, doi: 10.1142/S021800142352016X.

[20] Y. Gao, "A design of apparel appearance: Recognition and evaluation of clothing pattern styles under deep learning," The Leather and Textile Research Journal, vol. 110, pp. 1-12, 2023, doi: 10.31881/TLR.2023.110.

[21] J. Dustin, "Advancements in virtual garment simulation and digital fit analysis for custom fashion design," International Journal of Fashion Design Research and Development (IJFDRD), vol. 2, no. 1, pp. 1–7, 2025.

[22] K. Liu, X. Zeng, P. Bruniaux, et al., "Fit evaluation of virtual garment try-on by learning from digital pressure data," Knowledge-Based Systems, vol. 133, pp. 174–182, 2017, doi: 10.1016/j.knosys.2017.07.007.

[23] M. M. M. Nayak, M. N. Rani, K. Vaibhavi, M. Ashwinishree, and K. M. Suchithra, "AI fit-virtual clothing try on system using deep learning," IJCSE, vol. 9, no. 6, pp. 378–381, 2025.

[24] I. Kachbal and S. El Abdellaoui, "Computer vision for fashion: A systematic review of design generation, simulation, and personalized recommendations," Information, vol. 17, no. 1, pp. 11, 2025, doi: 10.3390/info17010011.

[25] H. Xu, J. Li, G. Lu, et al., "Predicting ready-made garment dressing fit for individuals based on highly reliable examples," Computers & Graphics, vol. 90, pp. 135–144, 2020, doi: 10.1016/j.cag.2020.06.002.

[26] W. Wang, H. I. Ho, C. Guo, et al., "4d-dress: A 4d dataset of real-world human clothing with semantic annotations," Proceedings of the IEEE/CVF Conference on Computer Vision and Pattern Recognition, pp. 550-560, 2024, doi: 10.1109/CVPR52733.2024.00059.